MECHANICAL BEHAVIOR OF FV535 STEEL AGAINST BALLISTIC IMPACT AT HIGH TEMPERATURES

B. Erice, F. Gálvez, D. Cendón and V. Sánchez-Gálvez.

Department of Materials Science, CISDEM, Polytechnic University of Madrid, Profesor Aranguren s/n, 28040, Madrid, Spain.

This paper presents the results of a wide experimental of ballistic tests against FV535 plates at temperatures from room to 700ºC. Those tests have been done using a light gas gun shooting round balls up to 800m/s. Residual velocity curves and the ballistic limit at different temperatures has been obtained. To check if the material model obtained from the Hopkinson bar tests reproduces the behavior of the material, the impact tests on FV535 plates are compared with numerical simulations. In those simulations the residual velocity curves have been compared with the experimental ones, introducing the Johnson-Cook fracture model in LS-DYNA explicit code.

The results shows that the model obtained reproduces very well the residual velocity curves. Taking a closer look at the impacted plates, and comparing the final geometry against the numerical simulations, the experimental and numerical geometries of the plates are almost identical. The special nature of these impact tests has been crucial to verify the Johnson-Cook fracture model

1. INTRODUCTION

The jet engine certification implies to ensure that in case of an accidental blade-off event all the fragments are contained by the casing and this should be guaranteed by the manufacturer. This certification needs to pass an experimental procedure that consists on an actual test of a full engine, where a blade is intentionally manipulated to fail. These kind of experimental procedures are hard to afford economically. Many resources are focused to improve and minimize the costs of these containment tests. So much so that future objective is to minimize these costs by making numerical simulations of the containment tests. Besides economical considerations, technical ones must be taken into account. The aerospace industry requires lightweight materials with high strength, in other words, a high strength/weight ratio. The material used in a turbine casing, besides the mentioned characteristics, must have a high temperature resistance. Having said that, the way to improve all these technical characteristics and obtain an optimal numerical simulation is to introduce a complete material model.

One of the most common materials used for jet engine turbine casings is the 9%-12% high chromium martensitic stainless steel, which has got excellent mechanical properties at relatively high temperatures and good corrosion resistance. The material used is the Firth-Vickers FV535 stainless steel. Numerical simulations with a real jet engine model are carrying out actually at the Department of Material Science in the Polytechnic University of Madrid. The explicit code chosen for that purpose is LS-DYNA in its 971 version. For the correct simulation of the complete impact phenomena produced inside the engine, it is necessary to introduce a material model that reproduces the more faithfully possible the real behavior of itself. Previous works [1,2] have shown that the Johnson-Cook material model [3] introduced in LS-DYNA numerical code, works reasonably well. The present work is then focused on obtaining a valid Johnson-Cook model for the material proposed

The accumulation of plastic strain is the basis of great majority of the fracture models. The Johnson-Cook model is not an exception. The standard procedure to obtain the Johnson-Cook fracture model is detailed in [3] and it has been used by Clausen et al. [4] or Børvik et al. [5] among others. This procedure is based on obtaining an equivalent plastic strain's fracture envelope which is triaxiality ratio, strain rate and temperature dependent. To get the values necessary to fulfill all the variables needed an extensive experimental programme is necessary. This programme includes axisymmetric rounded unnotched and notched specimens which will give us different values of the triaxiality ratio. To achieve this goal, a vast material characterization was done in this work. Quasi static and dynamic tensile tests of these specimens were performed to obtain the strain rate dependency. Eventually, tensile specimens at various temperatures were also tested.

The procedure implies using Bridgman's analysis [6] to evaluate the triaxiality ratio and the equivalent plastic strain to fracture. It has been demonstrated that Bridgman's analysis introduces notable errors and specially after specimens necking [8]. To avoid such errors, corrections, like the one applied by Mirone [9], for Bridgman's analysis have been applied with reasonable success. We have considered that the actual numerical codes have the capability to reproduce the specimens' tests and thus to obtain more accurate data to calibrate the fracture model. The present work details a methodology to calibrate Johnson-Cook fracture model. To validate the methodology, ballistic impact tests have been performed at various temperatures with a single stage gas gun. This has been possible thanks to the design in the shooting chamber of a ballistic furnace prototype. Simulations in LS-DYNA have been run for all the temperatures, to check the validity of the model.

2. MATERIAL

One of the most widely used materials for turbine casing is the FV535 high chromium (9%-12%) martensitic stainless steel. It has been received as a section of an original turbine casing and afterwards machined to produce the specimens.
In order to obtain the constants for the calibration of the JC fracture model three groups of experiments have been carried out. The first group of experiments includes quasi static tensile test at various triaxialities. The second one consists in dynamic tests at various triaxialities and the third group includes quasi static tests at various temperatures. Tablea 1 and 2 summarize the Johnson-Cook parameters derived from test results.

Table 1. Johnson-Cook material constitutive model for FV535 stainless steel from Gálvez et. al.[10]

A (MPa)	B (MPa)	C	n	m
1035	190	0.3	0.016	4.5

Table 2. Johnson-Cook fracture model's constants of the FV535 steel.

D_1	D_2	D_3	D_4	D_5
0.1133	45.5036	-4.2734	0.0125	0.6112

3. BALLISTICT TESTS

The aim of these tests is to validate the material model calibrated in previous section. The ideal situation to test the model is a ballistic impact test. Many researchers have used blunt nosed projectiles for this purpose, Teng and Wierzbicki [2], Dey et. al. [11] or Børvik et al. [12]. This type of projectile produces mostly a fracture caused by a very strong shear component. This means that the triaxiality values for the target material is not deeply involved in the fracture process. The ideal situation would be to produce a more complex stress state inside the target material. With this purpose instead of shooting blunt nosed projectiles, spherical projectiles have been chosen. The validation process involves also a specimen heating system, to test the material model at high temperatures.

A ballistic furnace prototype is presented in the current section. For the ballistic tests square plates of 101x101 mm with thicknesses of 2mm for FV535 steel have been tested. The projectile was a 5.55 mm diameter sphere of AISI 52100 bearing steel. The single stage gas gun system has a 7.62 mm caliber barrel. A polyethilene sabot was used to reach the barrel diameter. This gas gun can be fired with either air or helium depending on the top velocity needed. The desired initial velocity v_0 is achieved regulating the pressure in the gas chamber. Velocity measurements were taken with two different devices. The first one is located in the flight chamber and consists of two solid states optical window frames. The second device, which can be seen in Fig.1, consists of an electrically activated device specially designed for this purpose. This device emits an electrical signal when the projectile passes through the windows that are separated for a known distance. Table 3 summarizes all the experimental work done in the ballistic impact tests, as well as, the damage inflicted to each one of the plate specimens.
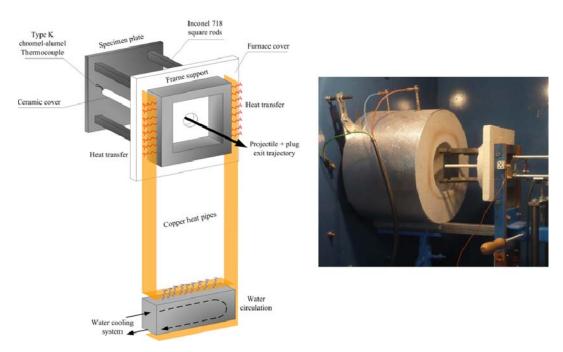

Fig.1. Detailed schematic view and some of the Ballistic furnace including the cooling system.

Table 3 - Results of the ballistic impact tests on FV535 plates at room temperature, 400 ºC and 700 ºC.

Temp (ºC)	Specimen Id.	Damage	Firing pressure	Impulse Gas	Initial velocity v_0 (m/s)	Residual velocity v_r (m/s)
700	FV535-36	Perforation	140 bar	Helium	719.6	449.2
	FV535-35	Perforation	80	Helium	595.8	319.2
	FV535-25	Perforation	60	Helium	490.1	214.8
	FV535-22	Perforation	80	Air	350.1	0.0
	FV535-23	Perforation	100	Air	379.5	0.0
	FV535-24	Perforation	125	Air	425.0	106.5
	FV535-21	Perforation	70	Helium	460.9	168.4
	FV535-20	Containment	100	Air	386.7	0.0
	FV535-19	Containment	110	Air	386.1	0.0
	FV535-18	Containment	120	Air	405.7	0.0
400	FV535-34	Perforation	120	Helium	661.2	319.6
	FV535-33	Perforation	80	Helium	600.0	298.4
	FV535-32	Perforation	70	Helium	554.7	-
	FV535-31	Perforation	200	Helium	753.5	-
	FV535-30	Containment	150	Air	422.4	0.0
	FV535-29	Containment	200	Air	457.4	0.0
	FV535-28	Perforation	60	Helium	530.4	210.5
	FV535-27	Containment	55	Helium	466.2	0.0
	FV535-25	Perforation	140	Helium	708.9	-
	FV535-17	Containment	60	Helium	472.9	0.0
	FV535-16	Perforation	180	Helium	672.2	331.0
	FV535-15	Perforation	70	Helium	511.8	158.7
	FV535-14	Perforation	200	Helium	795.4	455.7
24	FV535-13	Perforation	200	Helium	734.8	450.9
	FV535-12	Perforation	180	Helium	779.9	454.9
	FV535-11	Perforation	160	Helium	709.9	390.0
	FV535-10	Perforation	100	Helium	658.1	-
	FV535-09	Perforation	90	Helium	626.3	329.9
	FV535-08	Perforation	60	Helium	510.2	241.5
	FV535-07	Perforation	55	Helium	507.6	210.3
	FV535-06	Perforation	45	Helium	460.9	40.0
	FV535-05	Perforation	50	Helium	473.6	127.7
	FV535-04	Perforation	40	Helium	451.1	10.0
	FV535-03	Containment	40	Helium	430.0	0.0

There are many studies [11-16] that deal with similar problems to this one until this point. Even though, the case in which we are involved requires one more complexity, the temperature. The materials used for turbine blade containment are usually working at temperature above 400ºC. For this purpose a Ballistic furnace prototype has been designed and manufactured. The more notorious contribution to the work already done is the possibility offered by this device. Now, the ballistic impact tests can be performed at user desired temperature up to 800ºC.

The furnace must let pass through itself the projectile, for this reason it has been designed as a cylinder. The furnace is fixed to one of the testing chamber walls by one of its basis. The other basis, the one we can observe in Fig. 1, is mobile. This part is mounted in a rail to provide the correct manipulation of the target material plates. A thermocouple, connected to a furnace controller, selects the exact temperature of the plate. To avoid problems derived from too elevated temperatures outside the furnace, a cooling system has been also designed. A series of copper sheets acting as heat pipes have been placed around the rail mounted frame. These

sheets are in contact with a water circulation source. This way, there is no overheating of exterior component. Other problems may be caused by the accumulation of hot air inside the shooting chamber, thus installing a fan which renews the air inside the shooting chamber.

Authors like Forrestal et al. [17] and Børvik et al. [16] have proposed penetration models based on the approximation of quasi-static stress values. Such models predict the true radial compressive stress required to open a cylindrical cavity in a material depending on its different elastoplastic behavior. In the present work a more simplified penetration model have been adopted.

Børvik et al. [15], Arias et al. [14] and others use a modified version of Recht and Ipson's (MRI) relation (Eqn. 1).in which k_1 and k_2 are constants to be fitted with residual velocity data. The reason to use this modified equation are the multiple assumptions and previously adopted hypothesis, are not always fulfilled. In the previous calculation of the plug mass m we assume that is constant and also its volume is simplified. This can explain why we put k_1 as a corrector factor. Various are the reasons for correcting the equation adopting k_2 as the exponent. The shape of the projectile and the change of trajectory during the plate perforation are the most representative ones. Due to this, the modified Recht and Ipson's (MRI) relation is adopted.

$$v_r = k_1 \frac{\left(v_o^{k_2} - v_{50}^{k_2}\right)^{1/k_2}}{1 + m/M} \tag{1}$$

The results given in Table 3 are plotted in a residual velocity versus initial velocity curves in Fig. 3 respectively. The fit of these data is adjusted with the MRI fitting using the constants resumed in Table 4.

Table 4. Constants of MRI curve fit for experimental and numerical simulation data.

T (ºC)	m/M	Data	v_{50} (m/s)	k_1	k_2	Data	v_{50} (m/s)	k_1	k_2
24	0.0539	Experimental	440	0.81	1.90	Numerical	435	0.81	1.95
400			430	0.75	1.90		440	0.78	2.00
700			385	0.80	1.90		380	0.85	1.90

4. NUMERICAL SIMULATIONS

Three groups of numerical simulations have been carried out. One for each one of the ballistic impact tests temperatures. The objective of these simulations is to examine if the model obtained with the methodology detailed in the previous section is capable to match the experimental data.

2D axisymmetric simulations (Fig. 2) have been carried out in LS-DYNA v971. Approximately 64.172 shell elements have been used for the whole finite element model. We have chosen axisymmetric model because we considered that the shoot affected zone is far enough from the border, so the behavior of a square or circular plate would be the same. In other words the geometry of the plate is not significant in the shoot affected zone is far enough from the border. The border nodes of the target plate are fixed in x and y coordinates. Mesh element size is fundamental in penetration simulation of plates as it has been pointed out by Børvik et al.[15]. Ballistic limit prediction seems to be directly dependent on mesh size. In their

works Børvik et al. [15] and Dey et al. [18] use an element size of 100x100 μm^2 in the impact zone. The measured width of the cracks appeared in some plates after the tests, reveals that those cracks' width goes from 30 μm to 50 μm. It is reasonable to assume that smaller element sizes than the width of the cracks, will reproduce correctly the physical phenomena [19]. Hence, in the present work 20x20 μm^2 are used in the impact zone mesh. The step time is directly related with the characteristic length of the smallest element [35]. To avoid large calculation times a two transition zones to coarse elements far from the impact zone have been introduced. The last transition introduces an element size of 250x250 μm.

The material used for the target, which is the one we are interested in is the previously calibrated Johnson-Cook material model (Table 1 and Table 2). The contact algorithm used is *2D_AUTOMATIC_SINGLE_SURFACE without friction coefficients. Initial velocity condition has been applied to the projectile and then has been varied every 50 m/s from 800 m/s. The velocity goes every 50 m/s until the projectile is stopped and then in four or five runs the highest velocity without plugging is found. The results obtained are plotted in Fig. 3.
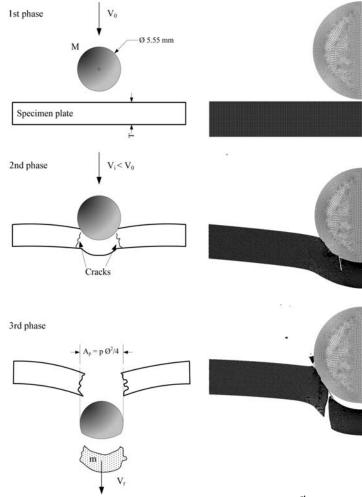

Fig. 2. Plate specimen material of FV535 impacted at v_0=600m/s. (1st phase) Left, schematic view of pre-impact phase and right, LS-DYNA finite element model. (2nd phase) Left, schematic view of contact phase between plate and projectile. Right, LS-DYNA capture of the same phase. (3rd phase) Left, schematic view of full penetration, and right, LS-DYNA capture of the same phase.

The initial versus residual velocity curves have been compared for each temperature with LS-DYNA simulations (Fig. 3). The results are summarized in Table 4. The curves show a good agreement between experimental and numerical data, even though, the size and the shape of the fracture in the plates, as well as the plugs and projectiles have not been analyzed.
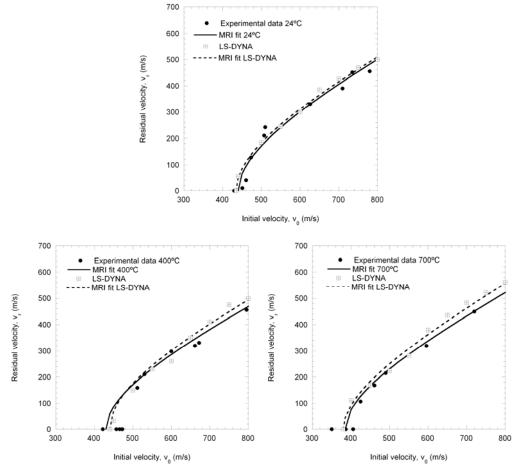

Fig. 3. Initial versus residual velocity curves for experimental data compared with LS-DYNA simulations at room temperature, at 400 ºC and 700 ºC.

5. CONCLUSIONS

In this work a numerical calibration methodology has been developed for the Johnson-Cook fracture model. This methodology has been applied for a specific case of the FV535 stainless steel and it is our aim to apply the same calibration methods for similar and different kind of materials. The objective of this work was to check if this methodology was able to calibrate correctly the model. The ballistic impact tests carried out for that purpose have been a good indicator of the model's calibration. Nevertheless, during the calibration some uncertainties have been faced. In the future more emphasis must be focused in the high temperature tests, the dispersion of the results can be determinant when matching the simulations with the experiments.

The last factor of the Johnson-Cook fracture model simplifies the fact that the fracture equivalent plastic strain's tendency with, almost in this case, is not linear.

In this case good results have been achieved but we must be aware that this could change significantly the behavior of the simulated material. The results for the calibrated model have been satisfying, although many simplifications have been done for 2D finite element models. The next step would be to complete full 3D LS-DYNA simulations of the ballistic test.

The modified Recht and Ipson's formulation has been found to fit the experimental and numerical data very well. At the same time the constants for the mentioned formulation are in good agreement between the experimental and the numerical data. Hence the ballistic limits are almost the same with an error lower than 5%.

References

[1] Børvik, T., Clausen, A. H., Eriksson, M., Berstad, T., Hopperstad, O. D.,and Langseth, M., Experimental and numerical study on the perforation of AA6005-T6 panels, International Journal of Impact Engineering, 32 (2005) 35-64.

[2] Teng, X., and Wierzbicki, T., Evaluation of six fracture models in high velocity perforation, Engineering Fracture Mechanics, 73 (2006) 1653-1678.

[3] Johnson, G.R., and Cook, W.H., Fracture characteristics of three metals subjected to various strains, strain rates, temperatures and pressures, Engineering Fracture Mechanics, 21 (1985) 31-48.

[4] Clausen, A.H., Børvik, T., Hopperstad, O. S., and Benallal, A., Flow and fracture characteristics of aluminium alloy AA5083-H116 as function of strain rate, temperature and triaxiality, Materials Science and Engineering, A364 (2004) 260-272.

[5] Børvik, T., Hopperstad, O. S., Dey, S., Pizzinato, E. V., Langseth, M., and Albertini, C., Strength and ductility of Weldox 460 E steel at high strain rates, elevated temperatures and various stress triaxilities, Engineering Fracture Mechanics, 72 (2005) 1071-1087.

[6] Bridgman, P.W., Studies in Large Flow and Fracture, McGraw-Hill, New York, 1952.

[8] Valiente, A., On Bridgman's Strees Solution for a Tensile Neck Applied to Axysimmetrical Blunt notched Tension Bars, Journal of Applied Mechanics, 68 (2001) 412-419.

[9] Mirone, G., Elastoplastic characterization and damage predictions under evolving local triaxility: axysimmetric and thick plate specimens, Mechanics of Materials, (2008) 685-694.

[10] Gálvez, F., Cendón, D., Enfedaque, A., and Sánchez-Gálvez, V., High strain rate and high temperature behaviour of metallic materials for jet engine turbine containment, Journal de Physique IV, 134 (2006) 269-274.

[11] Dey, S., Børvik, T., Hopperstad, O. S., and Langseth, M., On the influence of constitutive relation in projectile impact of steel plates, International Journal of Impact Engineering, 34 (2007) 464-484.

[12] Børvik, T., Hopperstad, O. S., Langseth, M., and Malo, K. A., Effect of target thickness in blunt projectile penetration of Weldox 460 E steel plates, International Journal of Impact Engineering, 28 (2003) 413-464.

[13] Arias, A., Rodríguez-Martínez, J. A., and Rusinek, A., Numerical simulations of impact behavior of thin steel plates subjected to cylindrical, conical and hemispherical non-deformable projectiles, Engineering Fracture Mechanics, 75 (2008) 1635-1656.

[14] Børvik, T., Langseth, M. , Hopperstad, O. S:, Malo, K. A. , Ballistic penetration of steel plates, International Journal of Impact Engineering, 22 (1999) 855-886.

[15] Børvik, T., Hopperstad, O. S., Berstad, T., and Langseth, M., Numerical simulation of plugging failure in ballistic penetration, International Journal of Solids and Structures, 38 (2001) 6241-6264.

[16] Børvik, T., Forrestal, M. J., Hopperstad, O. S., Warren, T. L., and Langseth, M., Perforation of AA5083-H116 aluminium pltes with conical-nose steel projectiles - Calculations, International Journal of Impact Engineering, 36 (2009) 426-437.

[17] Forrestal, M.J., Rosenberg, Z., Luk, V. K. and Bless, S. J. , Perforation of Aluminium Plates With Conical-Nosed Rods, Journal of Applied Mechanics, 57 (1987) 230-232.

[18] Dey, S., Børvik, T., Teng, X., Wierzbicki, T., and Hopperstad, O. S., On the ballistic resistence of double-layered steel plates: An experimental and numerical investigation, International Journal of Solids and Structures, (2007) 6701-6723.

[19] Dey, S., Børvik, T., Hopperstad, O. S., Leinum, J.R., and Langseth, M., The effect of target strength on the perforation of steel plates using three different projectile nose shapes, International Journal of Impact Engineering, 30 (2004) 1005-1038